Molecular Switches

International Edition: DOI: 10.1002/anie.201507688
German Edition: DOI: 10.1002/ange.201507688

Synthesis of a Neutral Mixed-Valence Diferrocenyl Carborane for Molecular Quantum-Dot Cellular Automata Applications

*John A. Christie, Ryan P. Forrest, Steven A. Corcelli, Natalie A. Wasio, Rebecca C. Quardokus, Ryan Brown, S. Alex Kandel, Yuhui Lu, Craig S. Lent, and Kenneth W. Henderson**

Abstract: *The preparation of 7-Fc^+-8-Fc-7,8-nido-$[C_2B_9H_{10}]^-$ ($Fc^+FcC_2B_9^-$) demonstrates the successful incorporation of a carborane cage as an internal counteranion bridging between ferrocene and ferrocenium units. This neutral mixed-valence Fe^{II}/Fe^{III} complex overcomes the proximal electronic bias imposed by external counterions, a practical limitation in the use of molecular switches. A combination of UV/Vis-NIR spectroscopic and TD-DFT computational studies indicate that electron transfer within $Fc^+FcC_2B_9^-$ is achieved through a bridge-mediated mechanism. This electronic framework therefore provides the possibility of an all-neutral null state, a key requirement for the implementation of quantum-dot cellular automata (QCA) molecular computing. The adhesion, ordering, and characterization of $Fc^+FcC_2B_9^-$ on Au(111) has been observed by scanning tunneling microscopy.*

The potential for electronic communication in mixed-valence compounds makes them attractive candidates as molecular switches within devices.[1] Indeed, incorporating molecular switches in the next generation of computing technologies, such as quantum-dot cellular automata (QCA), is a highly active area of study.[2,3] QCA relies on encoding binary information into quantum-dots or molecules by the location of an electron or hole (Figure 1). Implementation of QCA would overcome the power-wall that is pervasive in semiconductor-based computing. Proof-of-concept QCA experiments have been realized utilizing metallic nanometer-scale quantum-dots,[4] and our interest lies in extending this paradigm to the molecular realm. Desirable traits in a molecular switch include robust thermal and chemical properties, favorable surface organization, and multiple symmetric ground states. One current challenge is that mixed-valence compounds are normally comprised of selectively oxidized multi-metal systems, requiring the need for external counterions to achieve charge balance. Unfortunately, the external counterion has the possibility of biasing the potential ground states of the molecular switch.[3,5] To overcome this limitation, we sought the preparation of a neutral mixed-valence compound where the counterion is incorporated as part of the ligand backbone. Despite substantial interests in electron transfer processes, very few neutral mixed-valence compounds have been fully studied.[6–9]

Figure 1. A representation of bit information in a clockable QCA device. The dot indicates location of the mobile charge that determines the bit value. The "1" and "0" states are active states, encoding binary information, whereas the "null" state holds no information. An applied clocking field can shift between the null and active states.

The carborane 7-Fc^+-8-Fc-7,8-*nido*-$[C_2B_9H_{10}]^-$, $Fc^+FcC_2B_9^-$ (**3a**), was targeted since it combines several attractive features as a molecular switch for QCA applications. Specifically, the carborane unit carries a charge which balances that of the ferrocenium, the delocalized bonding in the carborane bridge potentially allows for electron transfer between the Fe^{II} and Fe^{III} centers, and finally, an all-neutral null state is possible. The null state, where the charge is symmetrically distributed as two ferrocenes and a neutral carborane, is an important element for microprocessor clocking in QCA.[10]

Scheme 1 details the successful synthetic route for the preparation of $Fc^+FcC_2B_9^-$ (**3a**) and the comparative monosubstituted derivative 7-Fc^+-7,8-*nido*-$[C_2B_9H_{11}]^-$, $Fc^+C_2B_9^-$ (**3b**). Insertion of the acetylenes FcC≡CR (R = Fc or H) into 6,9-$(Me_2S)_2$-*arachno*-$B_{10}H_{12}$ proceeds readily to form the dodecacarboranes 1-Fc-2-R-1,2-*closo*-$[C_2B_{10}H_{10}]$, R = Fc ($Fc_2C_2B_{10}$, **1a**) and H (FcC_2B_{10}, **1b**).[11] Base-mediated deboronation was accomplished using piperidine, followed by counterion exchange with $HNEt_3Cl$, to form the *nido*-carborane anions $Fc_2C_2B_9^-$ (**2a**) and $FcC_2B_9^-$ (**2b**). Finally, oxidation with a single equivalent of silver triflate produced the neutral mixed-valence compounds $Fc^+FcC_2B_9^-$ (**3a**) and $Fc^+C_2B_9^-$ (**3b**).

The molecular structures of the six carboranes were confirmed and compared by single-crystal X-ray diffraction analysis (Figure 2 and Supporting Information).[12,13] The Fe–C bond lengths in $Fc_2C_2B_{10}$ (**1a**), FcC_2B_{10} (**1b**), $Fc_2C_2B_9^-$ (**2a**), and $Fc_2C_2B_9^-$ (**2b**) fall in the narrow range 2.036(4)–

[*] J. A. Christie, R. P. Forrest, Dr. S. A. Corcelli, Dr. N. A. Wasio, Dr. R. C. Quardokus, Dr. R. Brown, Dr. S. A. Kandel, Dr. K. W. Henderson
Department of Chemistry and Biochemistry
University of Notre Dame
Notre Dame, IN 46556 (USA)
E-mail: kenneth.w.henderson.43@nd.edu
Dr. C. S. Lent
Department of Electrical Engineering
University of Notre Dame
Notre Dame, IN 46556 (USA)
Dr. Y. Lu
Department of Chemistry, Holy Cross College
Notre Dame, IN 46556 (USA)

Supporting information for this article is available on the WWW under http://dx.doi.org/10.1002/anie.201507688.

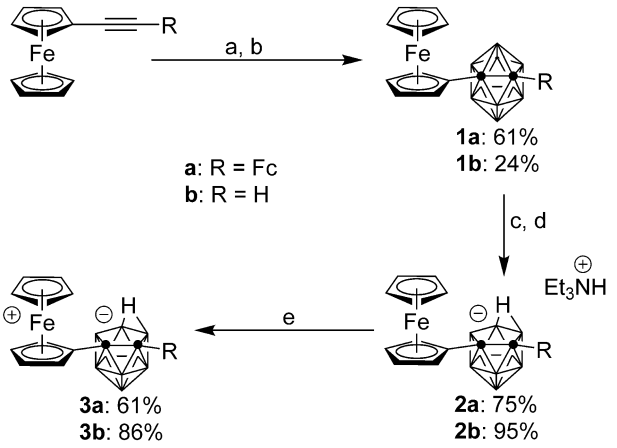

Scheme 1. Reagents and conditions: a) $B_{10}H_{14}$, SMe_2, 48 h; b) toluene, reflux, 16 h; c) piperidine, toluene, reflux, 6 days; d) CH_2Cl_2, $HNEt_3Cl$, 20 min; e) $AgSO_3CF_3$, CH_2Cl_2.

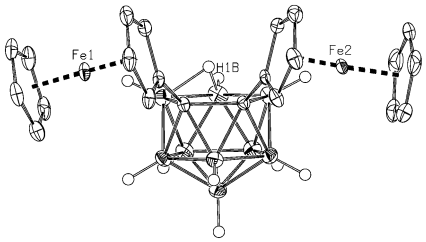

Figure 2. ORTEP plot of $Fc^+FcC_2B_9^-$ (**3a**) at 50% probability with solvent molecules omitted and only B–H hydrogen atoms shown for clarity.[29]

2.056(2) Å, consistent with Fe^{II} centers in ferrocenes.[14] In comparison, $Fc^+FcC_2B_9^-$ (**3a**) has one mean Fe–C length of 2.050(2) Å and a second longer mean length of 2.095(2) Å. Similarly, the mean Fe–C bond length in $Fc^+C_2B_9^-$ (**3b**) is 2.086(2) Å. These elongated Fe–C bonds are consistent with the formation of localized ferrocenium Fe^{III} centers in $Fc^+FcC_2B_9^-$ (**3a**) and $Fc^+C_2B_9^-$ (**3b**).[15–18] The C–C bond lengths within the cages shorten significantly on moving from the *closo* to the *nido* structures.[19] Specifically, the C11–C12 bond length within the *closo* compounds $Fc_2C_2B_{10}$ (**1a**) and FcC_2B_{10} (**1b**) are 1.763(2) and 1.653(2) Å respectively, whereas these lengths range between 1.553(3)–1.612(2) Å in the *nido* anions. In turn, any electronic communication between the metals may be affected by this change in the bridge. Also, it should be noted that the carborane is not perfectly symmetric as desired, with the bridging hydrogen, H1B, lying slightly towards the Fe^{II} center in $Fc^+FcC_2B_9^-$ (**3a**).

Having unambiguously determined the ability of $Fc^+FcC_2B_9^-$ (**3a**) to form a neutral mixed-valence species, its potential for intramolecular electronic communication was investigated. Electrochemical analysis of $Fc_2C_2B_9^-$ (**2a**) in methylene chloride reveals two reversible oxidation events at $E_{1/2} = -0.30$ V and $E_{1/2} = -0.08$ V, relative to the oxidation potential of ferrocene (Supporting Information). These events correspond to the formation of the mixed-valence Fe^{II}/Fe^{III} species, and the cationic Fe^{III}/Fe^{III} species, respectively. The 220 mV separation between oxidation events corresponds to a $K_c = 6.3 \times 10^3$.[20] As a consequence, there is only minor disproportionation from the Fe^{II}/Fe^{III} oxidation state to the Fe^{II}/Fe^{II} and Fe^{III}/Fe^{III} oxidation states in solution.

UV/Vis-NIR spectroscopy of $Fc^+FcC_2B_9^-$ (**3a**) in acetonitrile (Figure 3) shows a broad absorbance band at 11502 cm^{-1} that is absent in the spectrum of $Fc_2C_2B_9^-$ (**2a**).

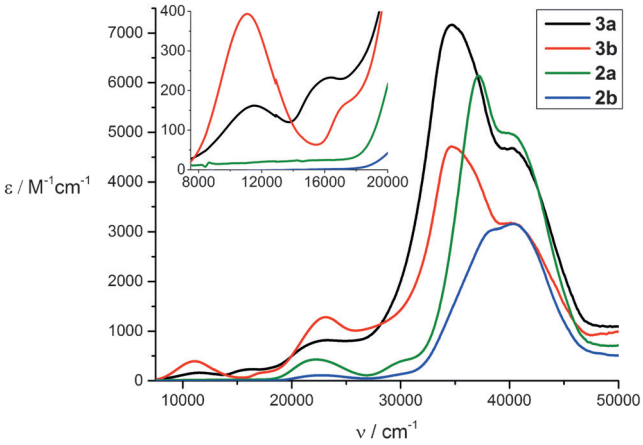

Figure 3. UV/Vis-NIR absorbance of $Fc_2C_2B_9^-$ (**2a**), $FcC_2B_9^-$ (**2b**), $Fc^+FcC_2B_9^-$ (**3a**), and $Fc^+C_2B_9^-$ (**3b**) in acetonitrile. The inset clearly shows the presence of the charge transfer band in both **3a** and **3b**.

This was pleasing, as it indicates that the presence of the ferrocenium enables some form of electronic communication within the molecule. To investigate the nature of this band, the monoferrocenyl compound $Fc^+C_2B_9^-$ (**3b**) was synthesized and characterized in an analogous fashion. The spectrum of $Fc^+C_2B_9^-$ (**3b**) in acetonitrile shows near-identical absorption features, with an absorbance band centered at 11156 cm^{-1} (Figure 3). This suggests that these signals in $Fc^+FcC_2B_9^-$ (**3a**) and $Fc^+C_2B_9^-$ (**3b**) correspond to a carborane-to-ferrocenium charge-transfer. This is consistent with a transient all-neutral state with a radical on the carborane cage (Figure 4). Interestingly, such a low-lying excited state is an appropriate null state for QCA clocking.

TD-DFT[21] calculations were performed to further investigate the nature of the charge-transfer process (Supporting Information). The calculations were performed using the PBE0[22,23] density functional with the def2-SVPD[24,25] basis set for all C, H, and B atoms and the def2-TZVPD[24,25] basis set for Fe atoms. Despite the occasional success of DFT in modeling weakly coupled ferrocene/ferrocenium mixed-valence system,[26] we observed charge delocalization when we attempted to model compounds **2a** and **3a**. Computations were therefore performed for monoferrocenyl systems $FcC_2B_9^-$ (**2b**) and $Fc^+C_2B_9^-$ (**3b**). This avoids the possibility of the positive charge being averaged over two locations in $Fc^+FcC_2B_9^-$ (**3a**) owing to the inherent self-interaction error found in DFT methods. The simulated spectra (Figure 5) were obtained by convoluting Gaussian functions with a standard deviation of 3250 cm^{-1} centered at the calculated excitation energies. The resulting spectra qualitatively approximate the experimental spectra, with $Fc^+C_2B_9^-$ (**3b**) displaying similar

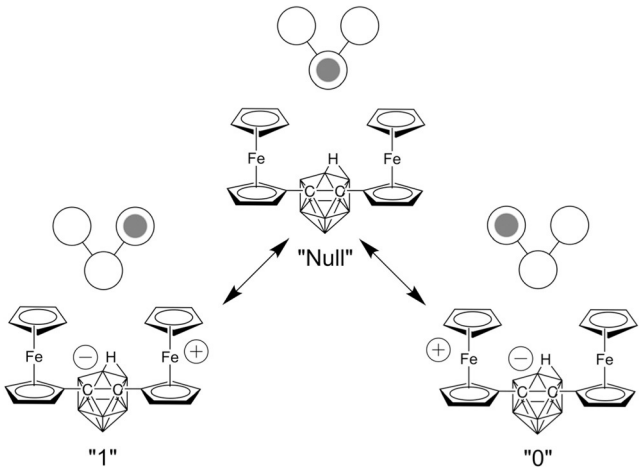

Figure 4. Bridge-mediated charge-transfer mechanism for the molecular switch $Fc^{+}FcC_2B_9^{-}$ (**3a**), highlighting the all-neutral null state intermediate.

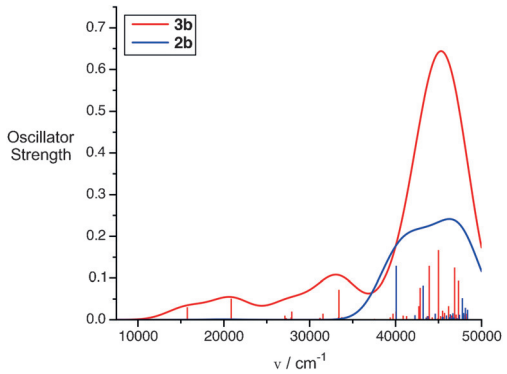

Figure 5. Calculated optically induced electronic transitions fit to a series of convoluted Gaussians for $FcC_2B_9^{-}$ (**2b**) and $Fc^{+}C_2B_9^{-}$ (**3b**).

features in the 7500 to 35000 cm^{-1} range, while $FcC_2B_9^{-}$ (**2b**) notably lacks features in this range. The first feature in the $Fc^{+}C_2B_9^{-}$ (**3b**) simulated spectrum is comprised of two convoluted excitations at 15757 and 20852 cm^{-1}. The TD-DFT results indicate that this is primarily a convolution of two excited states: a β-HOMO to β-LUMO electron transfer at 15757 cm^{-1}, and an α-HOMO to α-LUMO electron transfer at 20852 cm^{-1}. These orbitals are depicted in Figure 6. Both β-HOMO and α-HOMO orbitals are located on the carborane cage and both β-LUMO and α-LUMO orbitals are located on the ferrocenium. This supports a carborane to ferrocenium charge transfer assignment of the 11502 cm^{-1} feature in the experimental spectra (Figure 3).

A critical requirement for the successful implementation of molecular QCA is the ability to appropriately order molecules on surfaces.[27] As a first step in the process, we were successful in imaging a partial monolayer of $Fc^{+}FcC_2B_9^{-}$ (**3a**) using scanning tunneling microscopy (Figure 7). A single molecule consists of a large bright feature with two dimmer lobes, corresponding to the carborane cage and the two organometallic moieties, respectively. Moreover, $Fc^{+}FcC_2B_9^{-}$ (**3a**) is seen to zig–zag in rows, where each row has a bright

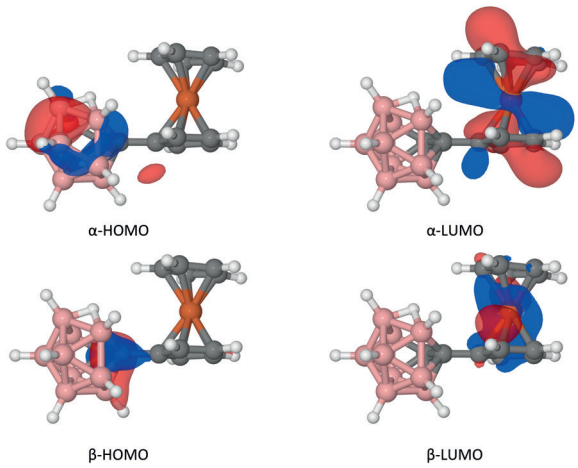

Figure 6. HOMO and LUMO orbitals relating to the cage to ferrocenium charge transfer for $Fc^{+}C_2B_9^{-}$ (**3b**).

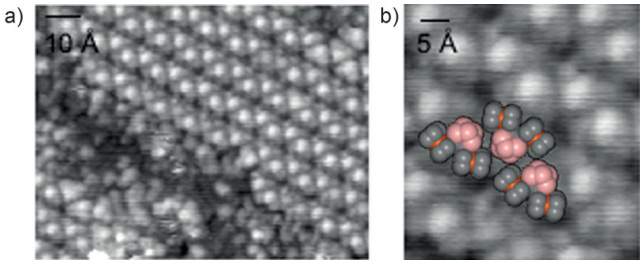

Figure 7. a) 147×113 Å STM image of $Fc^{+}FcC_2B_9^{-}$ (**3a**) scanned at a bias voltage of −1 V and 10 pA. Image was low-pass filtered to remove high frequency noise. b) Cropped and expanded 40×44 Å image with overlaid crystal structure data of **3a**.

carborane pointed inward and the ferrocenes pointed outward. These data indicate that not only is $Fc^{+}FcC_2B_9^{-}$ (**3a**) readily imaged at the molecular level, but that it orders in a manner where Coulomb interactions between neighbors may be achievable.

We have demonstrated that a *nido*-carborane can be employed as both an internalized counteranion in the preparation of neutral mixed-valence compounds, and as a useful bridging moiety to enable electronic communication between metal centers. The Fe^{II} to Fe^{III} electron transfer in $Fc^{+}FcC_2B_9^{-}$ (**3a**) is through a bridge-assisted mechanism involving an all-neutral null state.[28] The ability to form a null state within the molecule is essential for a viable QCA device. These characteristics, along with the surface ordering seen by STM, make $Fc^{+}FcC_2B_9^{-}$ (**3a**) a very attractive candidate for QCA, and further studies are currently in progress.

Acknowledgements

This work was supported by the US National Science Foundation under grant NSF CHE-1124762. The authors acknowledge high-performance computing resources and support from the Center for Research Computing at the University of Notre Dame.

Keywords: carboranes · mixed-valence compounds · QCA · STM · zwitterions

How to cite: *Angew. Chem. Int. Ed.* **2015**, *54*, 15448–15451
Angew. Chem. **2015**, *127*, 15668–15671

[1] Y. Lu, R. Quardokus, C. S. Lent, F. Justaud, C. Lapinte, S. A. Kandel, *J. Am. Chem. Soc.* **2010**, *132*, 13519 – 13524.
[2] C. S. Lent, B. Isaksen, M. Lieberman, *J. Am. Chem. Soc.* **2003**, *125*, 1056 – 1063.
[3] Y. Lu, C. S. Lent, *Chem. Phys. Lett.* **2013**, *582*, 86 – 89.
[4] I. Amlani, A. O. Orlov, G. Toth, G. H. Bernstein, C. S. Lent, G. L. Snider, *Science* **1999**, *284*, 289 – 291.
[5] Y. Lu, C. S. Lent, *Phys. Chem. Chem. Phys.* **2011**, *13*, 14928 – 14936.
[6] J. Ho, Z. Hou, R. J. Drake, D. W. Stephan, *Organometallics* **1993**, *12*, 3145 – 3157.
[7] A. Kudinov, D. Loginov, *Eur. J. Inorg. Chem.* **2002**, 3018 – 3027.
[8] J. C. Röder, F. Meyer, I. Hyla-Kryspin, R. F. Winter, E. Kaifer, *Chem. Eur. J.* **2003**, *9*, 2636 – 2648.
[9] For a review on organic neutral mixed-valance species see: A. Heckmann, C. Lambert, *Angew. Chem. Int. Ed.* **2012**, *51*, 326 – 392; *Angew. Chem.* **2012**, *124*, 334 – 404.
[10] A. O. Orlov, I. Amlani, R. K. Kummamuru, R. Ramasubramaniam, G. Toth, C. S. Lent, G. H. Bernstein, G. L. Snider, *Appl. Phys. Lett.* **2000**, *77*, 295.
[11] J. A. Kramer, D. N. Hendrickson, *Inorg. Chem.* **1980**, *19*, 3330 – 3337.
[12] A. Korotvička, I. Šnajdr, P. Štěpnička, I. Císařová, Z. Janoušek, M. Kotora, *Eur. J. Inorg. Chem.* **2013**, 2789 – 2798.
[13] C. Beckering, G. Rosair, A. Weller, *J. Organomet. Chem.* **1998**, *556*, 55 – 66.
[14] Y. L. Slovokhotov, *Cryst. Growth Des.* **2014**, *14*, 6205 – 6216.
[15] B. W. Sullivan, B. M. Foxman, *Organometallics* **1983**, *2*, 187 – 189.
[16] R. J. Webb, M. D. Lowery, Y. Shiomi, M. Sorai, R. J. Wittebort, D. N. Hendrickson, *Inorg. Chem.* **1992**, *31*, 5211 – 5219.
[17] N. J. Mammano, A. Zalkin, A. Landers, A. L. Rheingold, *Inorg. Chem.* **1977**, *16*, 297 – 300.
[18] S. Scholz, M. Scheibitz, F. Schödel, M. Bolte, M. Wagner, H.-W. Lerner, *Inorg. Chim. Acta* **2007**, *360*, 3323 – 3329.
[19] F. H. Allen, *Acta Crystallogr. Sect. B* **2002**, *58*, 380 – 388.
[20] R. F. Winter, *Organometallics* **2014**, *33*, 4517 – 4536.
[21] E. Runge, E. K. U. Gross, *Phys. Rev. Lett.* **1984**, *52*, 997 – 1000.
[22] J. P. Perdew, M. Ernzerhof, K. Burke, *J. Chem. Phys.* **1996**, *105*, 9982 – 9985.
[23] C. Adamo, G. E. Scuseria, V. Barone, *J. Chem. Phys.* **1999**, *111*, 2889 – 2899.
[24] F. Weigend, R. Ahlrichs, *Phys. Chem. Chem. Phys.* **2005**, *7*, 3297.
[25] D. Rappoport, F. Furche, *J. Chem. Phys.* **2010**, *133*, 134105.
[26] A. Hildebrandt, H. Lang, *Organometallics* **2013**, *32*, 5640 – 5653.
[27] M. Smeu, R. A. Wolkow, H. Guo, *J. Am. Chem. Soc.* **2009**, *131*, 11019 – 11026.
[28] C. Lambert, G. Nöll, J. Schelter, *Nat. Mater.* **2002**, *1*, 69 – 73.
[29] CCDC 1418833, 1418834, 1418835, and 1418836 contain the supplementary crystallographic data for this paper. These data can be obtained free of charge from The Cambridge Crystallographic Data Centre.

Received: August 17, 2015
Revised: September 21, 2015
Published online: October 30, 2015

